

Microstructures and Mechanical Properties of Mg-4.5Gd-2.6Nd-0.5Zn-0.5Zr New Casting Alloy

Zhan Liang^{1,2}, Le Qichi², Feng Zhijun¹, Lou Yanchun¹, Li Huawen³

¹ State Key Laboratory of Light Alloy Casting Technology for High-end Equipment, Shenyang Research Institute of Foundry Co. Ltd, Shenyang 110022, China; ² Key Lab of Electromagnetic Processing of Materials, Ministry of Education, Northeastern University, Shenyang 110819, China; ³ AECC Zhong Chuan Transmission Machinery Co. Ltd, Changsha 410200, China

Abstract: The microstructure and mechanical properties of Mg-4.5Gd-2.6Nd-0.5Zn-0.5Zr, a novel magnesium cast alloy, were investigated. The microstructure of the as-cast experimental alloy is determined to be composed of near-equiaxed α -Mg, Mg₁₂(Nd, Gd), and Mg₃Gd phases. After optimizing the heat treatment parameters, the YS, UTS, and *A* values reach 205 MPa, 325 MPa, and 4.0% at room temperature, and 145 MPa, 245 MPa, and 18.5% at 250 °C. The strengthening mechanism of this alloy was also investigated. The fracture surfaces of Mg-4.5Gd-2.6Nd-0.5Zn-0.5Zr during tensile tests demonstrate that brittle fracture occurs at room temperature, and ductile fracture occurs at 250 °C accompanied by appearance of many dimples and tear ridges.

Key words: Mg-4.5Gd-2.6Nd-0.5Zn-0.5Zr alloy; microstructure; mechanical properties

As one of the lightest current structural materials, magnesium alloys containing heavy rare earths (Mg-RE) have been applied in aerospace and automobile industries^[1-3]. However, the low strength and poor heat resistance of traditional magnesium alloys at high temperatures seriously limits their application in important industrial fields such as aviation, aerospace, military equipment, and automobiles^[4]. Strengthening magnesium alloys by introducing rare earths can be accomplished by a variety of methods, including secondary-phase (eutectic compounds) strengthening, solid solution strengthening, fine crystal strengthening, dispersion strengthening, and aging precipitation^[5]. Moreover, the solid solution, aging, and diffusion strengthening in magnesium by rare earth elements is more effective than in aluminum alloys^[6,7]. Strengthening by alloying with rare earths is an important method to improve the heat resistance and mechanical properties of magnesium alloys at high temperatures. The addition of multivariate rare earth composites is an effective method to strengthen rare earth alloys^[8,9]. Mg-Nd alloys have very attractive application prospects in aerospace, automotive racing, and electronics industries because of their excellent mechanical properties, thermal stability, and casting

performance. Gd has a more significant strengthening effect on magnesium alloys compared with Nd. Zn is an inexpensive alloy element, and magnesium alloys containing trace amounts of it possess excellent solid solution strengthening and age hardening effects. Referring to the ZM6 (Mg-Nd-Zn-Zr) alloy of China, we choose the Mg-4.5Gd-2.6Nd-0.5Zn-0.5Zr designed to study its microstructure and mechanical properties and also to develop a new high-strength heat-resistant magnesium cast alloy

1 Experiment

The elemental composition (wt%) of the test alloy was: Gd 4.2~4.7, Nd 2.5~3.0, Zn 0.4~0.7, and Zr 0.4~0.6, with the remainder composed of Mg. Alloy smelting was carried out under the protection of RJ-4 flux in a 12 kg resistance crucible furnace. The alloy was prepared from 99.99% Mg, 99.99% Zn, Mg-30%Gd, Mg-30%Nd, and Mg-30%Zr (wt%) master alloys. The melt was poured into a steel mold and pre-heated to 200 °C to form a tensile test bar at 750 °C by gravity casting. The results of the chemical composition analysis showed that the test alloy was composed of 4.5 Gd, 2.6 Nd, 0.5 Zn, and 0.5 Zr (wt%). The solid solution treatment of the alloy was carried

Received date: August 20, 2019

Corresponding author: Zhan Liang, Candidate for Ph. D., State Key Laboratory of Light Alloy Casting Technology for High-end Equipment, Shenyang Research Institute of Foundry Co. Ltd, Shenyang 110022, P. R. China, E-mail: srifal@163.com

Copyright © 2020, Northwest Institute for Nonferrous Metal Research. Published by Science Press. All rights reserved.

out in a quenched hot-air circulation furnace with a ± 2 °C temperature fluctuation, protected by FeS atmosphere. Samples were first heated to 350 °C and held for 30 min, and then raised to the solution-treatment temperature of 510, 520, or 530 °C until a specified time and then quenched in water at 60–80 °C. The quenching transfer time did not exceed 15 s. Alloy aging was carried out in an electric oven at 200, 225, and 250 °C.

Hardness testing of alloys was performed using a PH600 Brinell hardness tester. According to the minimum and maximum values, the average value of the remaining 3 hardness points was used as the final test result. All tensile tests were carried out on a CSS-1120 tensile testing machine equipped with an electric resistance furnace with a fully-enclosed chamber at 25–300 °C. The alloy microstructures were observed using an Olympus PM-G3 optical microscope (OM) and a JEOL JSM-5800 scanning electron microscope (SEM). X-ray diffraction (XRD) was performed on an X'Pert Pro MPD X-ray diffractometer. Microstructural examination was performed using a Sirion 200 field emission scanning electron microscope (FESEM), equipped with an Oxford energy-dispersive X-ray spectrometer (EDS). Transmission electron microscope (TEM) observations were performed using a JEM2100F operated at 200 kV.

2 Results and Discussion

2.1 Microstructure of the as-cast alloy

Fig. 1a shows the microstructure of the as-cast experimental alloy, which is composed of approximately equiaxed $\alpha(\text{Mg})$ grains and eutectic compounds at the grain boundary with a discontinuous netted lamellar eutectic phase. The SEM image of the as-cast test alloy in Fig. 1b suggests the alloy mainly contains two intermetallic phases, i.e. the network-shaped phase (marked by point A), and a blocky phase (marked by point B) along the grain boundary. In addition, the white dotted phase (marked by point C) in the $\alpha(\text{Mg})$ grains can be indexed to be $\alpha(\text{Zr})$. The typed particle were frequently observed in Mg-RE-Zn systems and have been reported to be Zr-rich particles or Zn-Zr compounds^[10,11].

The TEM images of precipitates within grains of the as-cast alloy are presented in Fig. 2. The blocky phase, marked as point B in Fig. 1b, appears to be composed of rod-shaped precipitates at high magnification in Fig. 2a. According to the SAED pattern shown in Fig. 2b, the dotted phase can be indexed to $\text{Mg}_{12}(\text{Nd}, \text{Gd})$ with a bcc structure. The network-shaped phase, marked as point A in Fig. 1b, is composed of network-shaped precipitates in the high magnification image in Fig. 3a. The SAED patterns of network-shaped precipitates are shown in Fig. 3b, and the network-shaped phase can be indexed to the Mg_5Gd phase with fcc structure^[10,11].

2.2 Microstructure of the solution-treated alloy

Based on the solution-treated temperature of the ZM6 alloy, solution treatment temperatures of 515, 520, and 530 °C were

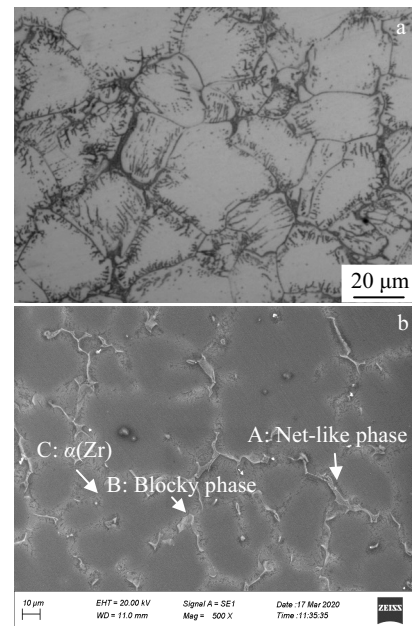


Fig.1 Optical micrograph (a) and SEM image (b) of the as-cast alloy

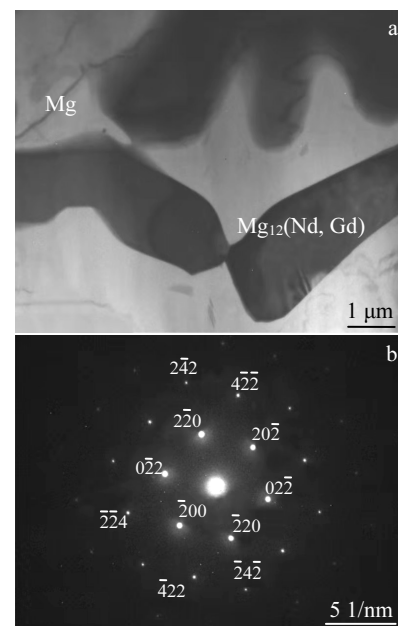


Fig.2 TEM bright field image (a) and SAED pattern (b) of the blocky precipitates within the α -Mg matrix

selected. After solution treatment at 515 °C for 16 h (Fig. 4a), some block phases form along the grain boundaries, as well as many fine α -Mg matrix precipitates. However, the average grain size increases to about 80 μm , which suggests that 515 °C for 16 h is insufficient for complete dissolution of the eutectic mixture.

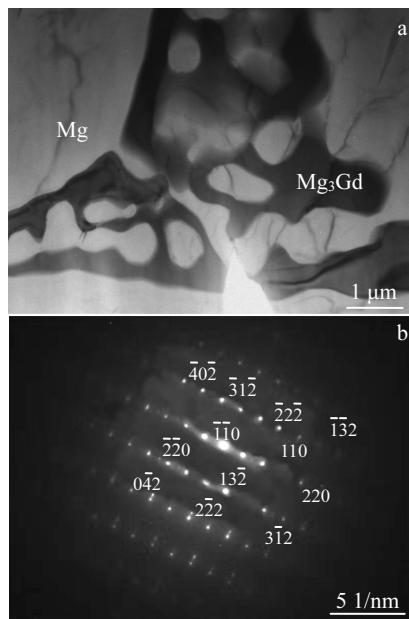


Fig.3 TEM bright field image (a) and SAED pattern (b) of the needle-like precipitates within the α -Mg matrix

After solution treatment at 520 °C for 12 h (Fig.4b), significantly fewer block phases are observed along the grain boundaries, together with much more fine precipitates compared with solution treatment at 515 °C for 16 h. Therefore,

520 °C for 12 h is also insufficient to complete the dissolution of the eutectic mixture. After solution treatment at 530 °C for 8 h (Fig.4c), all block phases are dissolved into the α -Mg matrix, with an average grain size of 55 μm . Further increasing the solid solution time to 10 h (Fig.4d) causes the grains to obviously coarsen, and the block phases decompose to fine block phases along the grain boundary. Therefore, the most suitable solid solution treatment of the alloy is determined to be 530 °C for 8 h.

2.3 Age hardening response

Fig.5 shows the age hardening curves for the alloy aged at 205, 225, and 250 °C. The specimen aged at 205 °C exhibited a peak hardness (HB) of 1050 MPa after aging for 16 h. When aged at 225 °C, a maximum hardness of 980 MPa was obtained after 4 h, while a peak hardness of 920 MPa was obtained only after 1.5 h when aging at 250 °C. The most suitable aging condition of the alloy was confirmed to be 205 °C for 16 h. The microstructure of the experimental alloy treated at 205 °C for 16 h in Fig.6a has obvious grain boundaries and cuboid compounds with sizes of approximately 0.5~3.0 μm , which appear as gray spots. More fine precipitates are observed to be uniformly distributed within the α (Mg) grains and along the grain boundaries than in the as-cast studied alloys. However, they contain fewer fine precipitates than the solution-treated sample, which has an average grain size of about 35 μm .

Fig.6a shows the SEM image of Mg-4.5Gd-2.6Nd-0.5Zn-0.5Zr alloy aged at 205 °C for 16 h. After the alloy was aged, the grain boundary became more obvious than the as-cast

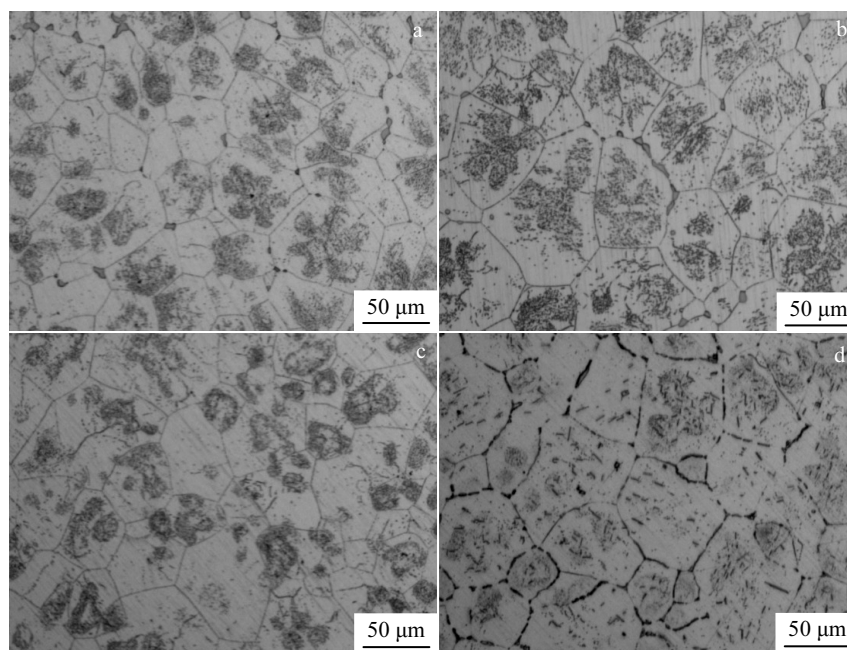


Fig.4 Optical micrographs of solution-treated alloy with different heat treatments: (a) 515 °C for 16 h, (b) 520 °C for 12 h, (c) 530 °C for 8 h, and (d) 530 °C for 10 h

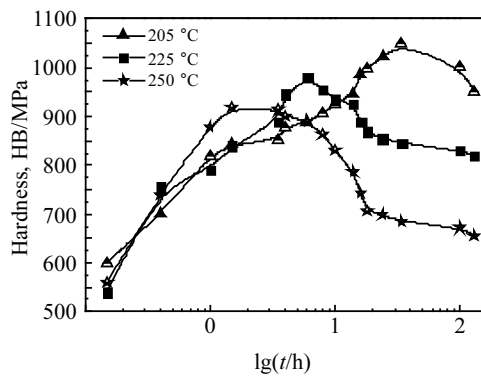


Fig.5 Hardness as a function of aging temperature for the solution-treated alloy

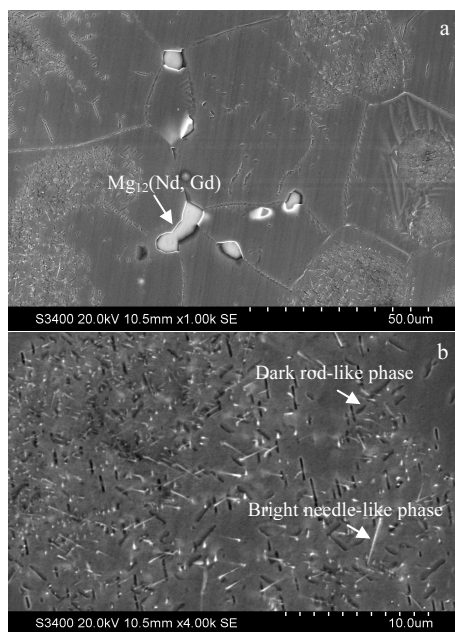


Fig.6 SEM images of the alloy aged at 205 °C for 16 h

alloy. The precipitated cuboidal phase along grain boundaries were determined to be $Mg_{12}(Nd, Gd)$. In addition, it was found that the clusters of precipitates are distributed within some $\alpha(Mg)$ grains and along grain boundaries, as shown in Fig.6a. The magnified SEM image in Fig.6b shows that the precipitates make up of the bright needle-like phases with different orientations. It was reported that the needle-like phases are Zn_2Zr_3 ^[12]. Moreover, some dark rod-shaped precipitates are distributed within some $\alpha(Mg)$ grains.

2.4 Mechanical properties

The mechanical properties, including the ultimate tensile strength (UTS), yield strength (YS), and elongation (A) of the as-cast (F), solution-treated (T4), and peak-aged (T6) alloy at room temperature presented in Fig.7 show that the as-cast alloy

has inferior mechanical properties. The UTS, YS, and A of the as-cast alloy are 195 MPa, 115 MPa, and 8.0%, respectively. After solution treatment, the UTS, YS, and A are 234 MPa, 128 MPa, and 11.0%, respectively, which indicates good strengthening and ductility. The UTS, YS, and A of the alloy are 325 MPa, 205 MPa, and 4.0% in the peak-aged specimen at room temperature. It is worth mentioning that the experimental alloy in the aging condition exhibits a much higher tensile strength and better ductility than WE43^[6] (4.2 wt% Y, 4.0 wt% RE, 0.5 wt% Zr) at 250 °C^[7], as shown in Table 1.

2.5 Fracture behavior

The SEM micrographs of the fracture behavior of the T6 experimental alloy after tensile tests at room temperature are shown in Fig.8a. The alloy exhibits some dimples, cleavage planes, and white cuboid-shaped residual phases containing many micro-cracks. EDS results show that the composition of the white cuboid-shaped residual phase is $Mg-6.10Nd-1.22Gd-0.12Zn$, indicating it has a similar composition to $Mg_{12}(Nd, Gd)$, in agreement with Fig.8c. This explains why the alloy has poor elongation during room temperature tensile tests. The SEM micrographs of fracture features of the T6 treated alloy after tensile test at 250 °C are shown in Fig.8b. The fracture surfaces of the experimental alloy contains more dimples and tear ridges than at room temperature, as well as a higher elongation.

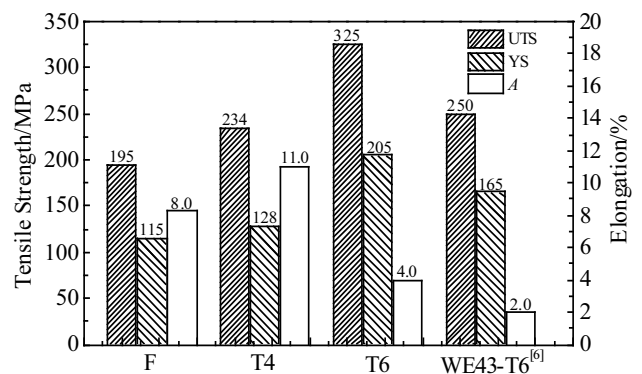


Fig.7 Mechanical properties of the experimental alloy at room temperature

Table 1 Tensile properties of the peak-aged Mg-4.5Gd-2.6Nd-0.5Zn-0.5Zr and WE43 alloy

Material	Test temperature/°C	YS/MPa	UTS/MPa	A/%
Mg-4.5Gd-2.6Nd-0.5Zn-0.5Zr	20	205	325	4.0
	250	145	245	18.5
WE43 ^[6]	20	165	250	2.0
	250	155	211	18.0

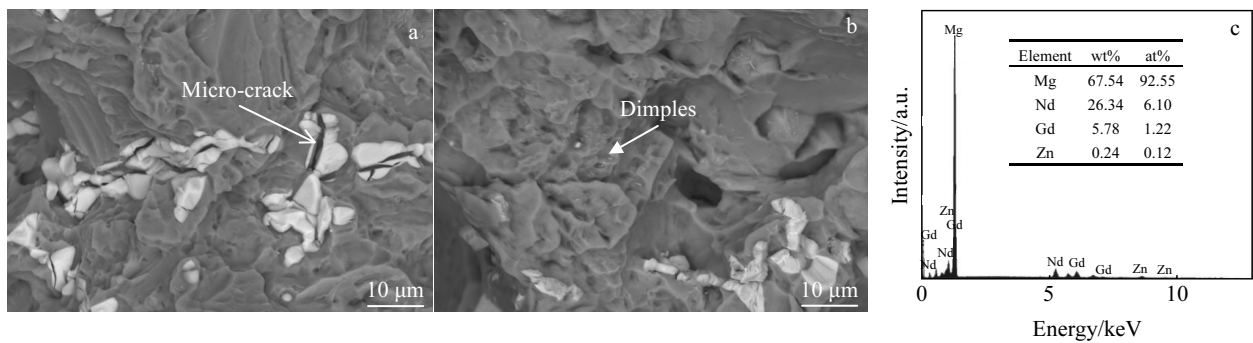


Fig.8 Tensile fracture morphologies of the T6 experimental alloy at room temperature (a) and 250 °C (b); EDS analysis of the cuboid-shaped phase (c)

3 Conclusions

1) The microstructure of the as-cast Mg-4.5Gd-2.6Nd-0.5Zn-0.5Zr (wt%) alloy is composed of an α (Mg) matrix, Mg_{12} (Nd, Gd) eutectic phases, Mg_3 Gd phase, and α (Zr) particles within the α (Mg) matrix.

2) For the experimental alloy, the optimum solid solution condition of the alloy is confirmed to be 530 °C for 8 h.

3) The Mg-4.5Gd-2.6Nd-0.5Zn-0.5Zr alloy exhibits intergranular fracture at room temperature.

4) The UTS, YS, and A of the alloy in the T6 are 325 MPa, 205 MPa, 4.0% at room temperature and 245 MPa, 145 MPa, and 18.5% at 250 °C, respectively. It is worth mentioning that the experimental alloy exhibits a much higher tensile strength and better ductility than WE43 at room temperature and 250 °C.

References

- 1 Su Zaijun, Liu Chuming, Wan Yingchun. *Materials and Design* [J], 2013, 45: 466
- 2 Joost W J, Krajewski P E. *Scripta Materialia*[J], 2017, 128: 107
- 3 Lou A A. *International Materials Reviews*[J], 2004, 49(1): 13
- 4 Li Shengyong, Li Dejiang, Zeng Xiaoqin et al. *Transactions of Nonferrous Metals Society of China*[J], 2014, 24(12): 3769
- 5 Xia X Y, Sun W H, Luo A A et al. *Acta Mater*[J], 2016, 111: 335
- 6 Yang Q, Qiu X, Lv S H et al. *Materials Science & Engineering A*[J], 2018, 716: 120
- 7 Xu Yongdong, Hu Shengsun, Li Song et al. *Rare Metal Materials and Engineering*[J], 2011, 40(7): 1133
- 8 Kim J M, Park J S. *Int J Cast Metal Res*[J], 2011, 24(2): 127
- 9 Wu X, Pan F S, Cheng R J et al. *Materials Science & Engineering A*[J], 2018, 726: 64
- 10 Riontino G, Massazza M, Lussana D et al. *Materials Science & Engineering A*[J], 2008, 494: 445
- 11 Nie J F, Muddle B C. *Scripta Mater*[J], 1999, 40(10): 1089
- 12 Liu S J, Yang G Y, Luo S F et al. *Materials Characterization*[J], 2015, 107: 334

新型 Mg-4.5Gd-2.6Nd-0.5Zn-0.5Zr 铸造合金的显微组织和力学性能

占 亮^{1,2}, 乐启焱², 冯志军¹, 姜延春¹, 李华文³

(1. 沈阳铸造研究所有限公司 高端装备轻合金铸造技术国家重点实验室, 辽宁 沈阳 110022)

(2. 东北大学 材料电磁过程研究教育部重点实验室, 辽宁 沈阳 110819)

(3. 中国航发中传机械有限公司, 湖南 长沙 410200)

摘 要: 对新型 Mg-4.5Gd-2.6Nd-0.5Zn-0.5Zr 铸造合金的显微组织和力学性能进行了研究。发现合金的铸态组织由近等轴晶、 Mg_{12} (Nd, Gd)和 Mg_3 Gd 合金组成。通过最优化热处理后, 合金的室温和高温 250 °C 时的屈服强度、抗拉强度和延伸率分别为 205 MPa, 325 MPa 和 4.0%; 145 MPa, 245 MPa 和 18.5%。同时研究了合金的强化原则。合金室温下断裂为脆性断裂, 高温下为韧性断裂。高温下断裂特征具有很多韧窝和撕裂脊。

关键词: Mg-4.5Gd-2.6Nd-0.5Zn-0.5Zr 合金; 微观组织; 力学性能

作者简介: 占 亮, 男, 1985 年生, 博士生, 沈阳铸造研究所有限公司高端装备轻合金铸造技术国家重点实验室, 辽宁 沈阳 110022, E-mail: srifal@163.com